



~~77533~~  
~~8~~

*Montgomery L. M. Knight*

~~1~~

TECHNICAL NOTES

NATIONAL ADVISORY COMMITTEE FOR AERONAUTICS

\_\_\_\_\_  
No. 336  
\_\_\_\_\_

THE EFFECT OF WING TIP FLOATING AILERONS ON  
THE AUTOROTATION OF A MONOPLANE WING MODEL

By Montgomery Knight and Carl J. Wenzinger  
Langley Memorial Aeronautical Laboratory

**FILE COPY**

To be returned to  
the files of the Langley  
Memorial Aeronautical  
Laboratory

Washington  
March, 1930

NATIONAL ADVISORY COMMITTEE FOR AERONAUTICS.

---

TECHNICAL NOTE NO. 336.

---

THE EFFECT OF WING TIP FLOATING AILERONS ON THE AUTOROTATION  
OF A MONOPLANE WING MODEL.

By Montgomery Knight and Carl J. Wenzinger.

S u m m a r y

The preliminary tests described in this report were made in order to determine the extent to which wing tip floating ailerons might be effective in reducing airplane spinning tendencies. In these tests the ailerons were in the neutral position and rigidly interconnected, and the model was set at zero yaw. Autorotation rates and rolling moments were measured on an autorotation dynamometer in the atmospheric wind tunnel of the Langley Memorial Aeronautical Laboratory. Although yaw (or sideslip) may be expected to modify the results, the tests show that initial spinning tendencies and rates of stable spinning could doubtless be reduced by the use of such ailerons on an airplane. It also appears desirable to reduce to a minimum the interference between wing and aileron in order to maintain uniformity of action at all angles of attack and to enable calculation of the aileron characteristics. A simplified method of calculation is included.

### Introduction

Improvements in airplane safety appear to be possible with the use of floating ailerons. This type of aileron is of value not only from the standpoint of effectiveness in stalled flight, but also by reason of its property, when in neutral, of reducing the tendency of an airplane to spin. It is to be pointed out that this property is separate and distinct from the functioning of such ailerons as control surfaces.

In principle the device consists of an airfoil surface mounted in the vicinity of each wing tip and balanced both statically and aerodynamically about a lateral axis so that it may align itself with the relative wind when the lateral control is in neutral. Operation of the control turns one surface up and the other down, and a rolling moment is thus produced (References 1, 2, and 3). In addition, if the two surfaces are rigidly interconnected by a suitable linkage, their action when in the neutral position is such as to oppose the rolling tendencies that are characteristic of airplane wings in stalled flight. A preliminary study of this latter feature of these ailerons is the purpose of this report.

A simple explanation of the reduction of rolling or spinning tendencies by means of floating ailerons can be given by neglecting the flow interference effects between the ailerons and the wing. In Figure 1, two floating airfoil surfaces whose

chords are parallel are shown rigidly connected by a rod, which is also the axis about which the surfaces are balanced and free to align themselves as a unit with the wind. X-X is an axis in the plane of symmetry and parallel to the wind direction about which the rolling motion may be considered to occur, as is generally the case in wind tunnel autorotation tests. The aerodynamic conditions thus obtained approximate those of the spin.

Let us now suppose that the wing and ailerons are in rotation. If  $y$  be the distance from the axis X-X to the mid-span point of each aileron, then for the direction of rotation designated by the circular arrow, i.e., right aileron moving downward, the effective wind velocity  $V_E$ , at this point will be the vector sum of  $V$ , the general wind velocity, and  $V_R$ , the wind velocity component due to the rotation (where  $V_R = p y$  and  $p =$  angular velocity). The latter component is opposite in direction, of course, for each aileron as shown. The mean effective angles of attack for down- and up-going ailerons are  $+\Delta\alpha$  and  $-\Delta\alpha$ , respectively. Due to these angles of attack at which the respective ailerons operate, forces are produced which are approximately normal to the general wind direction, the force on the down-going aileron being up and that on the up-going aileron being down. It is thus evident that the rolling motion is opposed by the ailerons, and that the addition of such surfaces to the wings of an airplane might be expected to

reduce its spinning tendencies.

A more careful analysis of the problem calls for a study of the interference effects due to the proximity of wing and ailerons. That these effects may not be negligible when floating ailerons are displaced to produce rolling moments, has been demonstrated in Reference 3, and it may also be expected that interference will modify the effectiveness of the floating surfaces in reducing spinning tendencies. The writers know of no information that has been published on this point hitherto.

In the very limited time that has, thus far, been available to devote to this problem at the Langley Memorial Aeronautical Laboratory, a few autorotation dynamometer tests have been made in the 5-foot atmospheric wind tunnel (Reference 4). Analysis of the test data showed that the autorotation rates and maximum autorotational rolling moments of the wing were considerably reduced when the floating surfaces were added, and it was felt that, in spite of the limited scope of the tests, the information was of sufficient interest to warrant publication.

#### Apparatus

The wing model with the floating ailerons was one that had been used in previous force tests made to determine the rolling and yawing moments and the changes in lift and drag produced by such ailerons. The results of these former tests have already been published (Reference 3). The wing model, exclusive

of ailerons, was a rectangular airfoil of 30-inch span and of 4.94-inch chord, and had a symmetrical profile, the ordinates of which are given in the above reference. The rectangular ailerons each had a span of 4 inches and the same profile and chord as the wing. They were attached at the wing tips so as to form a continuation of the wing, and the gap between wing and aileron was about .015 inch. The axis of rotation was located on the chord line 1.16 inches (23.5 per cent chord) back from the leading edge. A steel rod extending through the wing in a slot connected the two ailerons which were fixed upon it. The surfaces were statically balanced and together with the rod were free to turn as a unit in small plain bearings mounted at each end of the wing.

Since it is intended to publish a detailed description of the autorotation dynamometer in a later report, only a brief explanation will be given here. This apparatus consists of a ball bearing shaft parallel to the air stream driven through reduction gearing by a small electric motor. The motor and gearing are mounted at the rear of the shaft in a cradle supported on knife edges located on the shaft center line. An arm attached to the cradle at right angles to the knife edges is connected by a suitable linkage to a balance outside the tunnel upon which the rolling moments for rotations in either direction are measured. The dynamometer assembly is housed in an aluminum fairing as shown in Figure 2, which is a view of the tunnel installation.

In these tests the wing was mounted on the dynamometer shaft extension arm as shown. A simple clamp arrangement permitted the angle of attack to be varied as desired. The rate and direction of rotation were controlled by a variable speed motor with a reversing switch, used in conjunction with a stroboscopic tachometer.

When making the stable autorotation tests mentioned below, the model was allowed to turn freely. This was accomplished by merely disengaging the reduction gearing.

#### T e s t s

The tests were divided into two groups:

1. Wing only.
2. Wing with neutral floating ailerons.

Both stable autorotation and rolling moment tests were made on each model arrangement.

In the stable autorotation tests the model was arranged to rotate freely as explained above and the rates of rotation at various angles of attack  $\alpha_m$ , were measured. In addition, the angles of attack between which the model would start rotating of itself and also those angles at which it just did not rotate when given a start by hand, were observed.

The rolling moment tests were made with the dynamometer gearing in mesh so that the speed of rotation could be controlled by means of the motor. Torques due to the rotation were measured

at various rotation rates for various angles of attack.

The tests were made at a dynamic pressure of 4.05 pounds per square inch, corresponding to an average air speed of 58.4 feet per second or 39.8 m.p.h. The Reynolds Number was about 148,000.

### R e s u l t s

The results are presented as absolute coefficients in both tabular and curve form. The curves are faired through points representing the mean values obtained for rotation of the model in both directions and cover the following variables:

1. Autorotation rates versus angle of attack both with and without ailerons (Fig. 3).
2. Rolling moments due to rolling versus rate of rotation both with and without ailerons (Fig. 4).
3. Difference between rolling moments with and without ailerons versus rate of rotation (Fig. 5).

The coefficients were obtained as follows:

$$C_p = \frac{p b}{2 V}$$

where

- $C_p$  = absolute coefficient of rotation,  
 $p$  = angular velocity,  
 $b$  = span of wing (exclusive of ailerons),  
 $V$  = wind velocity,

and where

$$C_\lambda = \frac{\lambda}{q b S},$$

- $C_\lambda$  = absolute coefficient of rolling moment,



$\lambda$  = measured rolling moment about dynamometer axis,  
 $S$  = area of wing (exclusive of ailerons),  
 $q$  = dynamic pressure.

In general, the measured data as tabulated may be considered accurate to within  $\pm 3$  per cent. The rates of stable autorotation were not corrected for the friction of the ball bearings, but this error is probably not greater than  $-2$  per cent. Torque readings were corrected for bearing friction, windage of the model arm, and for asymmetry in the model. The angle of attack settings were accurate to about  $\pm 0.2$  degree.

In order to show the approximate magnitude and sense of the interference effects between wing and ailerons, the moments produced by the neutral ailerons (without the wing) while rolling  $C_{\lambda_R}$ , have been calculated by a simple method. These calculated results are given in Figure 5, together with the experimentally determined values which are the moment differences for the wing with and without ailerons.

Certain simplifying approximations are made in these calculations. In the first place, during rotation the variation in effective angle of attack along the aileron span is very nearly linear and hence the angle  $\Delta\alpha$ , at  $y$  (see Fig. 1) may be considered to be a mean value. Moreover, lift and normal force on the ailerons are practically equal in magnitude up to the angle of attack of maximum lift. We then find that the damping in roll produced by the ailerons without the wing is:

$$\begin{aligned}\lambda_a &= q y S_a C_L, \\ &= q y S_a \left( \Delta \alpha \frac{d C_L}{d \alpha} \right)\end{aligned}\quad (1)$$

where  $\lambda_a$  = aileron rolling moment,  
 $S_a$  = area of both ailerons,  
 $\frac{d C_L}{d \alpha}$  = slope of aileron lift curve.

This moment may be written in the usual form of absolute coefficient with reference to the wing as

$$\begin{aligned}C_{\lambda_a} &= \frac{\lambda_a}{q b S} \\ &= \frac{y S_a}{b S} \left( \Delta \alpha \frac{d C_L}{d \alpha} \right)\end{aligned}\quad (2)$$

where  $C_{\lambda_a}$  = absolute coefficient of aileron rolling moment.  
 $C_{\lambda_a}$  may be more conveniently expressed in terms of  $C_p$ , as defined above, in the following manner:

$$\text{Since } \tan \Delta \alpha = \frac{p y}{V},$$

$$\begin{aligned}\text{and } C_p &= \frac{p b}{2 V} \\ \Delta \alpha &= \tan^{-1} \left( 2 C_p \frac{y}{b} \right)\end{aligned}$$

and hence

$$C_{\lambda_a} = \frac{y S_a}{b S} \tan^{-1} \left( 2 C_p \frac{y}{b} \right) \frac{d C_L}{d \alpha}\quad (3)$$

For values of  $C_D$  up to 0.2, angle and tangent are practically the same and equation (3) may be reduced to

$$C_{\lambda_a} = 2 \frac{y^2 S_a}{b^2 S} C_D \frac{d C_L}{d \alpha} \quad (4)$$

A further simplification arises from the fact that  $\frac{d C_L}{d \alpha}$  may be considered practically constant up to  $C_D = 0.15$ , since the lift curve is very nearly a straight line up to about  $0.9 C_{L \max}$ . Hence, for the range of rotation of Figure 5, it is sufficiently accurate to solve equation (4) for one value of  $C_D$  only and to draw a straight line through this point and the origin. The value of  $\frac{d C_L}{d \alpha}$  used in this calculation is 1.72 ( $\alpha$  in radians).

#### Discussion

The spinning rate of an airplane is indicated approximately by stable autorotation tests. Figure 3 shows that the addition of the floating ailerons to the wing reduced the maximum rate of autorotation to about one-third of its original value. Moreover, the range of angles of attack over which the rotation was self-starting was reduced from 6 degrees to  $1\frac{1}{2}$  degrees, and the maximum range over which autorotation could be made to occur was reduced from about 9 degrees to  $2\frac{1}{2}$  degrees. The dashed portions of the curves in Figure 3 are estimated, since the apparatus was not capable of measuring rates of unstable autorotation, and are included merely to show the trend.

The rapidity with which an airplane will go into a spin is roughly indicated by the magnitude of the positive (autorotational) rolling moments as determined on the autorotation dynamometer. A marked reduction in autorotational moments was produced by the floating ailerons as indicated in Figure 4. In these curves also the dashed portions are estimated values, where the dynamometer operation became unstable. However, it was possible, in general, to measure the maximum positive moments, since instability did not set in until slightly lower rates of rotation had been reached. The large increase in negative (damping) moments due to the ailerons is noteworthy.

Figure 5 is of interest in that it indicates to what extent the mathematically predicted characteristics of the floating ailerons were modified by interference effects. A comparison of the solid and dashed lines shows that below the stall ( $\alpha_m = 10$  degrees) interference approximately doubles the damping moments due to the ailerons alone. On the other hand, above the stall ( $\alpha_m = 14$  degrees and 18 degrees) up to a value of  $C_p$  of about 0.12, interference reduces these damping moments, although beyond this point the reverse is true. It will be noted that, in general, the experimental results for 14 degrees and 18 degrees correspond more closely with the calculated values than do those for 10 degrees.

Damping in roll below the stall is generally quite sufficient in conventional airplanes. Moreover, it is particularly

desirable to have the damping moments due to the floating ailerons above the stall as large as possible, especially at the lower rates of roll which are representative of the incipient spin. It would, therefore, appear advisable to reduce the interference to a minimum, thereby approaching the condition shown by the calculated curve in Figure 5. This reduction in interference could probably be accomplished by increasing the gap between the wing and the ailerons, or by rounding the adjacent tips of wing and ailerons in plan.

An airplane when spinning is also usually sideslipping to some extent. Recent tests made at this laboratory with a wing model set on the autorotation dynamometer at various angles of yaw have shown that sideslip produces large rolling moments at angles of attack beyond that of maximum lift. This effect may be expected to modify the action of floating ailerons as tested under the symmetrical conditions described in this report. A study of sideslip will be part of a later extended investigation on such ailerons to be conducted at this laboratory. This study will also include tests on a wing with ailerons modified to reduce interference as suggested above.

## Conclusions

1. Rigidly interconnected floating ailerons, when in the neutral position, may be expected to reduce both the initial spinning tendency of an airplane and also the rate of rotation in the stable spin.

2. It appears to be desirable to reduce interference between the wing and the floating ailerons as much as possible in order to obtain uniform action at all angles of attack, and also to enable calculation of the aileron characteristics.

Langley Memorial Aeronautical Laboratory,  
National Advisory Committee for Aeronautics,  
Langley Field, Va., February 19, 1930.

## References

1. Bradfield, F. B.  
and  
Peatfield, I. L. : Lateral Control at Low Speeds. British A.R.C. Reports and Memoranda No. 717 (1920).
2. Bradfield, F. B.  
and  
Simmonds, O. E. : Rolling and Yawing Moments Due to Roll of Model Avro Wings with Standard and Interplane Ailerons and Rudder Moments for Standard and Special Large Rudder. British A.R.C. Reports and Memoranda No. 848 (1922).
3. Knight, Montgomery  
and  
Bamber, Millard J. : Wind Tunnel Tests on a Model of a Monoplane Wing with Floating Ailerons. N.A.C.A. Technical Note No. 316 (1929).
4. Reid, Elliott G. : Standardization Tests of N.A.C.A. No. 1 Wind Tunnel. N.A.C.A. Technical Report No. 195 (1924).

TABLE Ia. Stable Autorotation Test.

Wing without Ailerons

$\alpha^\circ$	Positive rotation	Negative rotation
	$C_p$	$C_p$
13	0	.137
14	.158	.172
15	.182*	.196*
16	.207*	-
17	.210*	.223*
18	.219*	.227*
20	.215*	.223*
21	.193	.196
22	.201	0

\*Self-starting.

TABLE Ib. Stable Autorotation Test  
Wing with Ailerons

$\alpha^\circ$	Positive rotation	Negative rotation
	$C_p$	$C_p$
15.3	.072	.066*
16.3	.076*	.067*
17.3	0	.057*
18.3	0	0

\*Self-starting.

TABLE IIa. Rolling Moment Test-Wing without Ailerons  
 $\alpha = 10^\circ$

Positive rotation		Negative rotation	
$C_p$	$C_\lambda$	$C_p$	$C_\lambda$
.079	-.0317	.067	-.0270
.113	-.0435	.103	-.0409
.232	-.0459	.245	-.0482
.277	-.0545	.297	-.0598
.319	-.0644	.348	-.0740



TABLE IIa. Rolling Moment Test-Wing without Ailerons (cont.)  
 $\alpha = 14^\circ$ 

Positive rotation		Negative rotation	
$C_p$	$C_\lambda$	$C_p$	$C_\lambda$
.093	-.0125	.113	+.0101
.205	-.0053	.203	-.0053
.268	-.0200	.248	-.0160
.319	-.0347	.297	-.0239
.370	-.0535	.361	-.0511
.412	-.0690	.422	-.0708

 $\alpha = 18^\circ$ 

Positive rotation		Negative rotation	
$C_p$	$C_\lambda$	$C_p$	$C_\lambda$
.127	-.0092	.112	+.0090
.241	-.0029	.247	-.0037
.319	-.0211	.305	-.0170
.373	-.0376	.348	-.0295
.446	-.0616	.415	-.0510
		.482	-.0740

TABLE IIb. Rolling Moment Test-Wing with Ailerons  
 $\alpha = 10^\circ$ 

Positive rotation		Negative rotation	
$C_p$	$C_\lambda$	$C_p$	$C_\lambda$
.036	-.0393	.043	-.0467
.055	-.0562	.057	-.0593
.071	-.0709	.074	-.0757

 $\alpha = 14^\circ$ 

Positive rotation		Negative rotation	
$C_p$	$C_\lambda$	$C_p$	$C_\lambda$
.126	-.0303	.129	-.0332
.143	-.0421	.154	-.0512
.160	-.0547	.184	-.0731
.183	-.0705		

TABLE IIb. Rolling Moment Test-Wing with Ailerons (cont.)  
 $\alpha = 15.3^\circ$ 

Positive rotation		Negative rotation	
$C_p$	$C_\lambda$	$C_p$	$C_\lambda$
.048	-.0010	.060	+.0055
.057	-.0019	.085	-.0035
.061	-.0010	.098	-.0089
.062	-.0024	.121	-.0218
.095	-.0149	.125	-.0248
.123	-.0329	.150	-.0386
.132	-.0384	.172	-.0552
.0155	-.0541	.186	-.0655

 $\alpha = 17.3^\circ$ 

Positive rotation		Negative rotation	
$C_p$	$C_\lambda$	$C_p$	$C_\lambda$
.050	-.0036	.067	+.0027
.064	-.0054	.093	-.0044
.078	-.0086	.116	-.0163
.105	-.0194	.161	-.0396
.132	-.0342		
.161	-.0520		

TABLE IIb. Rolling Moment Test-Wing with Ailerons (cont.)  
 $\alpha = 18^\circ$ 

Positive rotation		Negative rotation	
$C_p$	$C_\lambda$	$C_p$	$C_\lambda$
.071	-.0070	.066	-.0096
.112	-.0188	.105	-.0209
.142	-.0324	.140	-.0367
.170	-.0469	.168	-.0503
.199	-.0618		

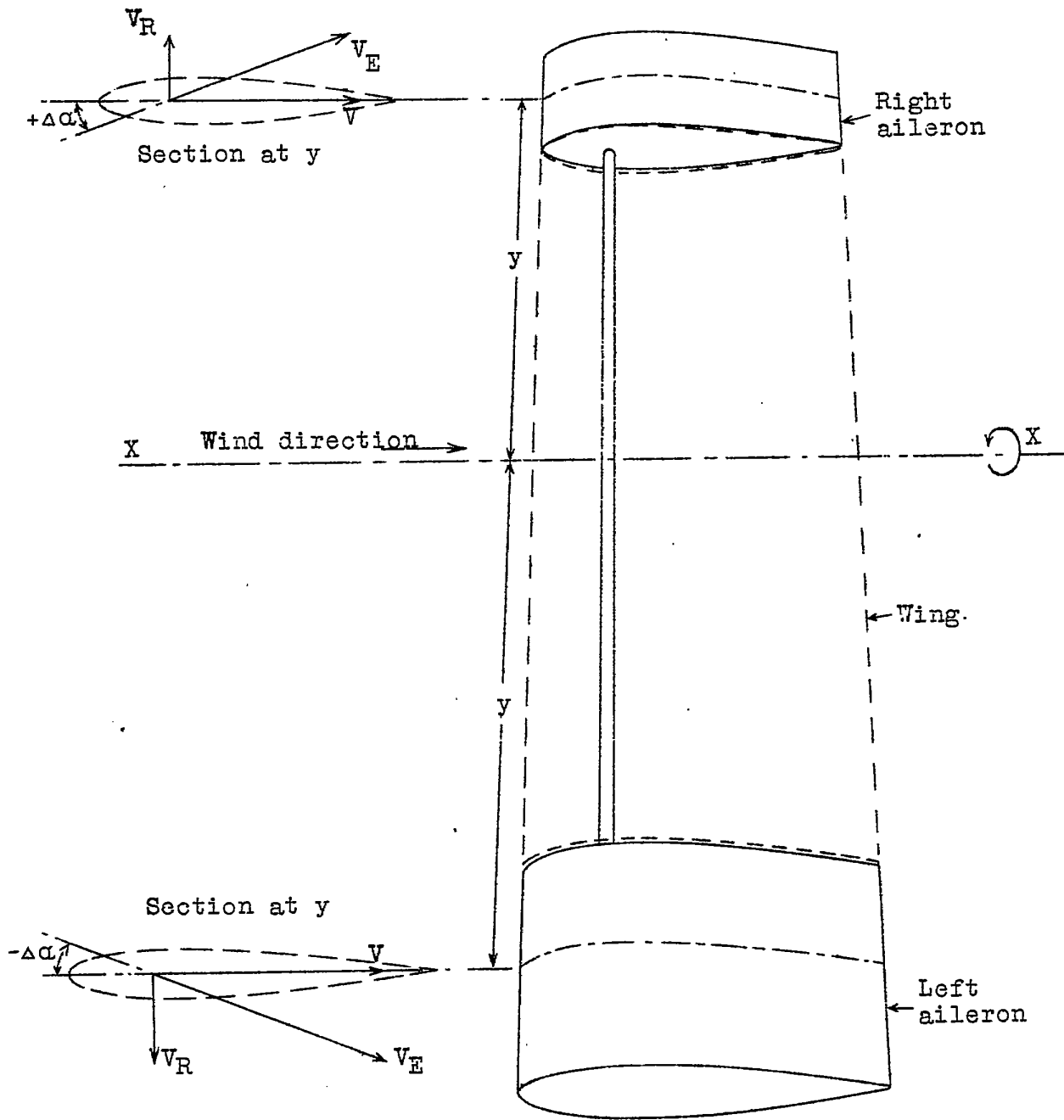


Fig.1 Diagram illustrating principle of operation of wing tip floating ailerons.

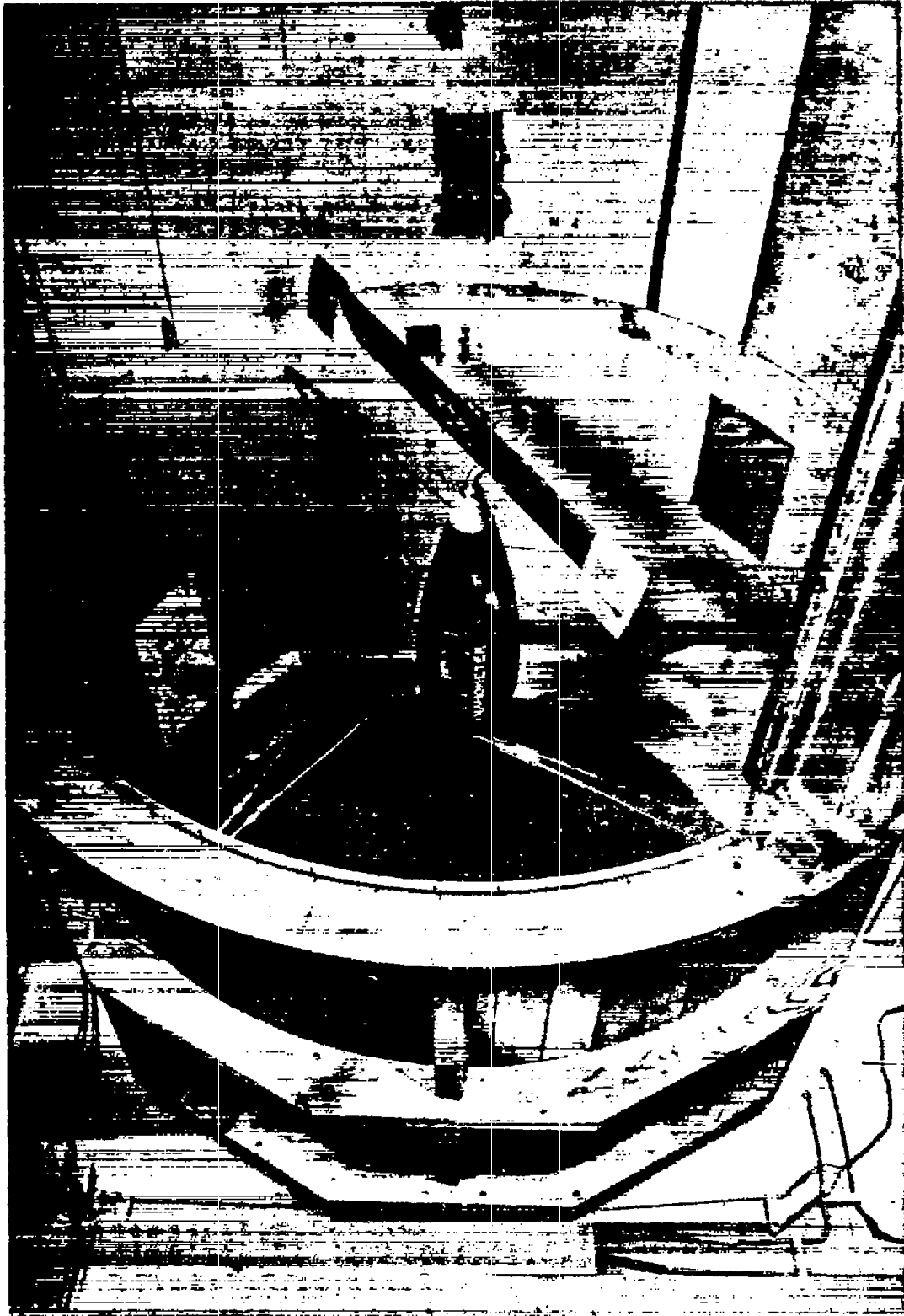


Fig.3 Wind tunnel installation of autorotation dynamometer and wing model.

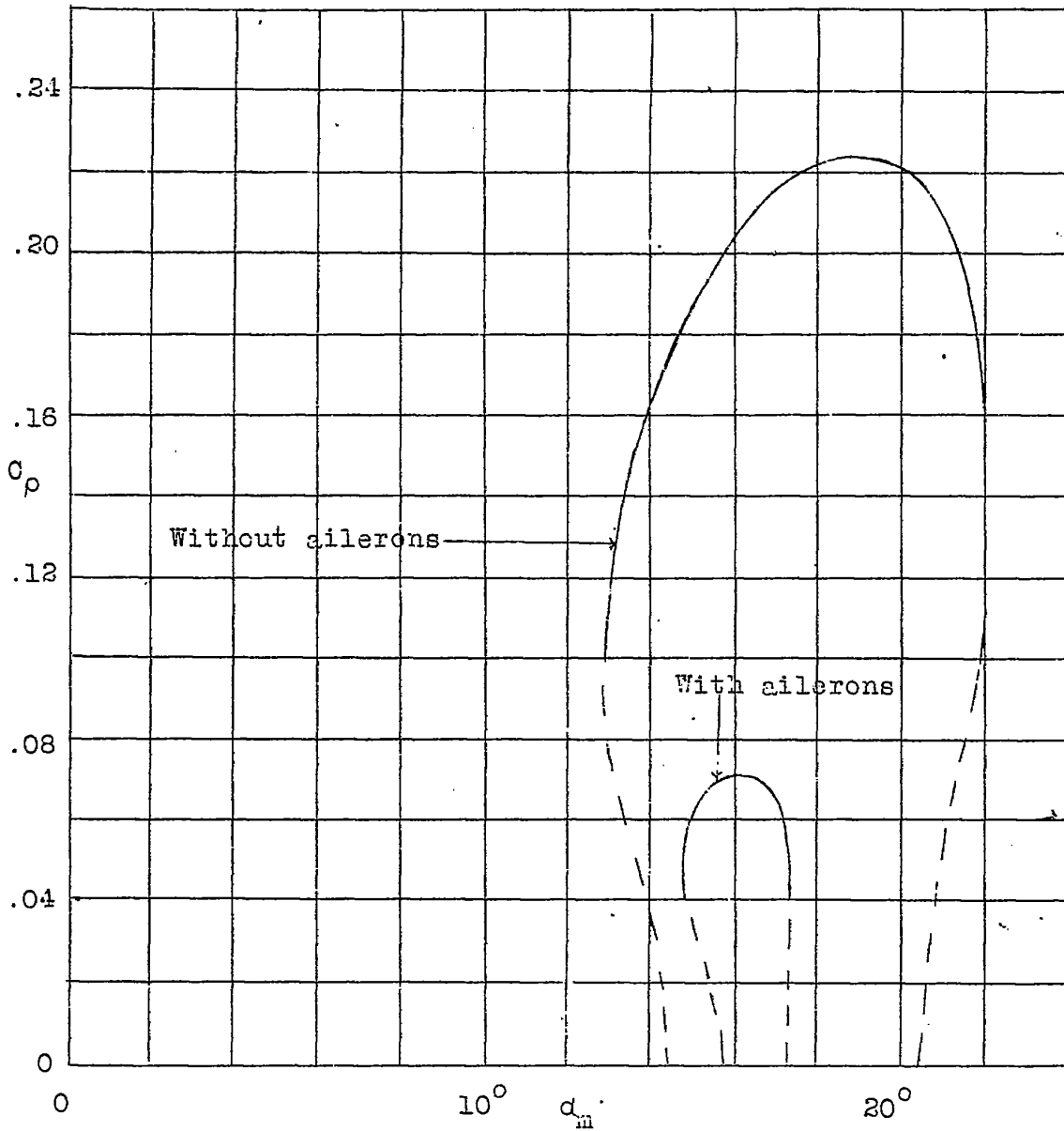


Fig. 3 Rate of autorotation vs. angle of attack.

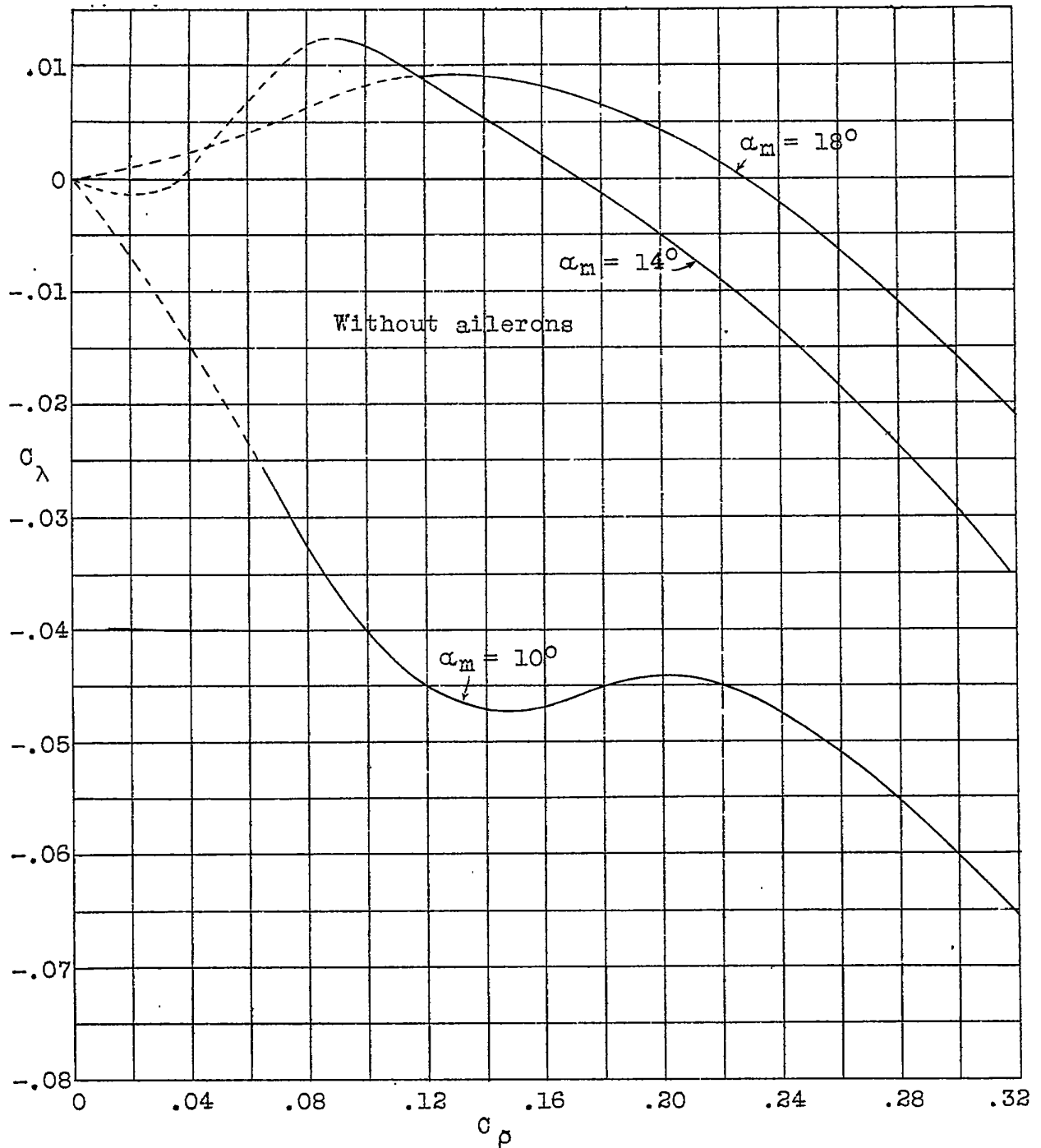
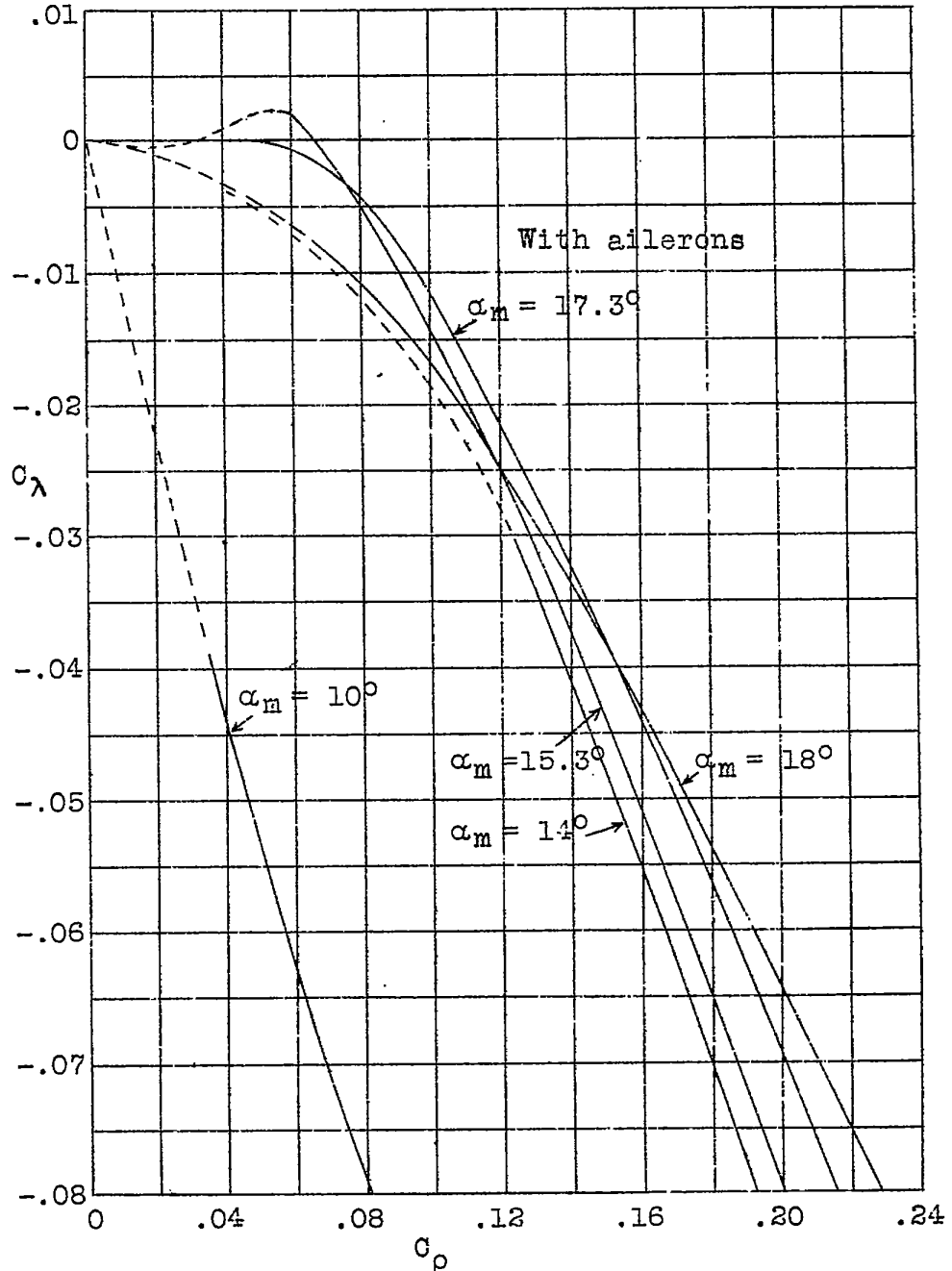


Fig.4 Rolling moment due to rolling vs. rate of rotation.  
 (Continued on next page.)





Continuation of Fig.4

Rolling moment due to rolling vs. rate of rotation.

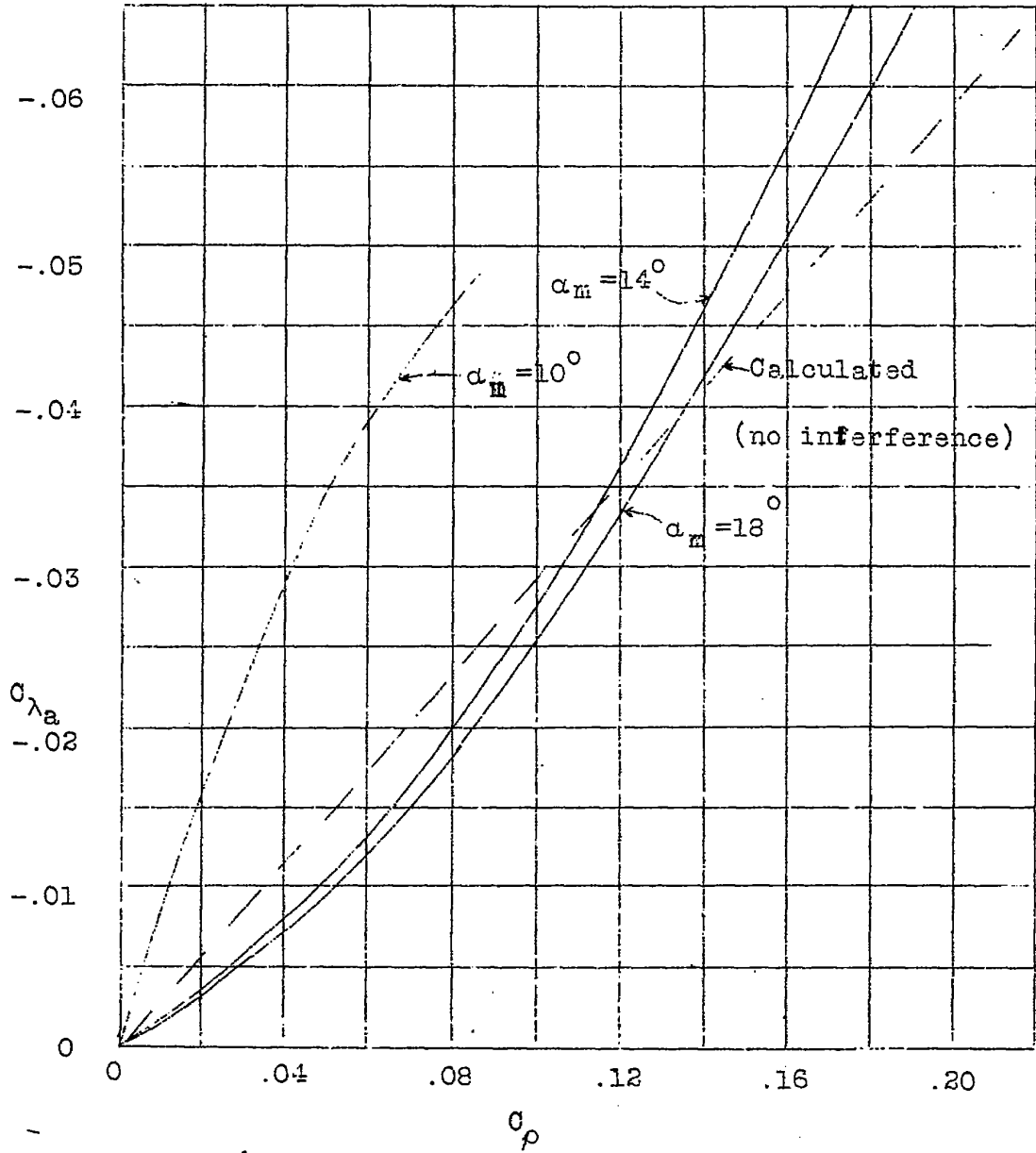


Fig. 5 Difference between rolling moments with and without ailerons vs. rate of rotation.